

# Spontaneous emission mediated by cooperative energy transfer to plasmonic antenna

Tigran V. Shahbazyan

Department of Physics, Jackson State University, Jackson, MS 39217 USA

Spontaneous emission from ensembles of quantum emitters (QEs) such as atoms, molecules, or semiconductor quantum dots can be greatly accelerated due to cooperative behavior arising from electromagnetic correlations between them. We describe new cooperative emission mechanism mediated by cooperative energy transfer (CET) from QEs to localized surface plasmon in metal-dielectric structure. The transferred energy is radiated away by the plasmonic antenna at rate that equals the sum of individual QE emission rates. For large QE ensembles saturating the plasmon mode volume, we derive universal, i.e., independent of local field distribution, expression for cooperative Purcell factor that far exceeds the field enhancement limits for individual QE in a hot spot. We also derive radiated power spectrum that retains the plasmon resonance lineshape and, in contrast to common cooperative mechanisms, is insensitive to natural variations of QEs' emission frequencies.

Surface plasmons are collective electronic excitations that can be resonantly excited in metal-dielectric structures with characteristic size well below the diffraction limit [1]. Rapid oscillations of electron charge density at metal-dielectric interfaces generate extremely strong alternating local fields that can dramatically affect optical properties of nearby dye molecules or semiconductor quantum dots, hereafter referred to as quantum emitters (QEs) [2–5]. Optical interactions between QEs and plasmons give rise to a number of major phenomena such as surface-enhanced Raman scattering (SERS) [6], plasmon-enhanced fluorescence and luminescence [7–9], plasmon-assisted energy transfer [10–13], strong QE-plasmon coupling [14–20] and plasmonic laser (spaser) [21–23].

Plasmonic enhancement of spontaneous emission from a QE near plasmonic structure is a generic effect that underpins much of plasmon-enhanced spectroscopy phenomena and many plasmonics applications [24–30]. The enhancement is rooted in highly efficient energy transfer (ET) from QE, located in the strong local field region, to localized plasmon in metal-dielectric structure followed by plasmon radiative decay (antenna effect) [31–37]. The local field enhancement of decay rate, usually described by the Purcell factor [38], can reach several orders of magnitude, e.g., near sharp metal tips, but is still limited by Ohmic losses in metal and nonlocal effects [40, 41].

On the other hand, light emission from *ensemble* of QEs can be greatly accelerated by cooperativity stemming from electromagnetic correlations between QEs. A prominent example is Dicke superradiance of QEs interacting with common radiation field to form collective states that radiate at a rate proportional to the ensemble size [42, 43]. When QEs are placed near plasmonic structure, radiation coupling between QEs is strongly enhanced by plasmon local fields [44–51] thus reducing negative impact of direct dipole interactions [52, 53]. At the same time, the Ohmic losses suppress correlations between QEs close to the metal surface, i.e., where the local fields are strongest [44, 45]. Notwithstanding recent reports [54, 55], observation of plasmon-enhanced superradiance remains a challenge as it hinges on delicate interplay between direct coupling, plasmonic correlations, and metal losses.

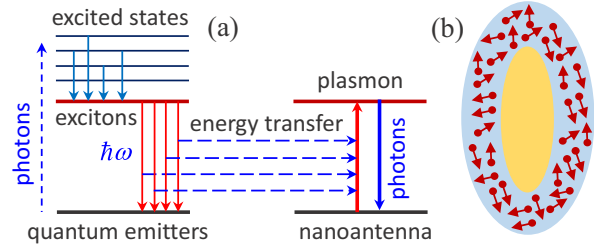


FIG. 1. (a) Schematics of CET from QE ensemble to plasmonic antenna. (b) Schematics of plasmonic system with QEs distributed within dielectric shell surrounding metallic core.

In this paper, we describe new mechanism of cooperative emission based on *cooperative energy transfer* (CET) from ensemble of QEs to plasmonic antenna (see Fig. 1). We demonstrate that excited QEs resonantly coupled to a single plasmon mode form collective state that transfers its energy cooperatively to plasmon at rate equal to the sum of individual QE-plasmon ET rates. The transferred energy is radiated away by the plasmonic antenna at rate that, while restricted by plasmon's radiation efficiency, scales with the number of QEs involved in CET process. We derive the cooperative Purcell factor describing plasmonic enhancement of the ensemble decay rate and show that, for QEs saturating plasmon mode volume, it has universal form independent of local field distribution in metal-dielectric structure. We derive explicit expression for radiated power spectrum, which retains the plasmon resonance lineshape with overall amplitude proportional to the cooperative Purcell factor.

Importantly, the CET mechanism is insensitive to natural QE frequency variations due to, e.g., direct dipole-dipole interactions, as long as the QE frequency spread fits within broad plasmon absorption band. Such spectral stability stays in stark contrast with common cooperative mechanisms, such as superradiance, where even weak disorder strongly alters the emission spectra [52, 53], and, combined with decay rate enhancement, is highly relevant for device applications [27–30]. Below we outline our theory for CET-based cooperative emission and present numerical results pointing that cooperative rate enhancement exceeds by far the local field enhancement limits.

*Theory.*—We start with spontaneous decay of *single* QE coupled to a plasmonic resonator represented by metal-dielectric nanostructure characterized by complex dielectric function  $\varepsilon(\omega, \mathbf{r}) = \varepsilon'(\omega, \mathbf{r}) + i\varepsilon''(\omega, \mathbf{r})$ . We assume that characteristic system size is much smaller than the radiation wavelength so that the plasmon electric field  $\mathbf{E}(\mathbf{r})$ , which we chose to be real, and frequency  $\omega_{pl}$  satisfy the quasistatic Gauss law  $\nabla \cdot [\varepsilon'(\omega_{pl}, \mathbf{r}) \mathbf{E}(\mathbf{r})] = 0$  with standard boundary conditions [5]. The decay rate of QE located at  $\mathbf{r}_0$  is given by  $\gamma = (2/\hbar) \text{Im}[\mathbf{p}^* \cdot \mathbf{E}(\mathbf{r}_0)]$ , where  $\mathbf{E}(\mathbf{r}) = \bar{\mathbf{D}}(\omega; \mathbf{r}, \mathbf{r}_0) \cdot \mathbf{p}$  is the electric field of QE's oscillating dipole  $\mathbf{p} e^{-i\omega t} = \mu \mathbf{n} e^{-i\omega t}$ , where  $\mu$  and  $\mathbf{n}$  are dipole moment and orientation, respectively, and  $\bar{\mathbf{D}}(\omega; \mathbf{r}, \mathbf{r}') = (4\pi\omega^2/c^2) \bar{\mathbf{G}}(\omega; \mathbf{r}, \mathbf{r}')$  is the electromagnetic Green function ( $\bar{\mathbf{G}}$  is the standard dyadic Green function for Maxwell equation including plasmonic system [56]).

In the *near field* limit, the Green function can be split into free-space and plasmon parts,  $\bar{\mathbf{D}} = \bar{\mathbf{D}}_0 + \bar{\mathbf{D}}_{pl}$ , and accordingly, the QE decay rate has the form  $\gamma = \gamma_0^r + \gamma_{et}$ , where  $\gamma_0^r = 4\mu^2\omega^3/3\hbar c^3$  is free-space decay rate [56] and

$$\gamma_{et} = \frac{2\mu^2}{\hbar} \text{Im} [\mathbf{n} \cdot \bar{\mathbf{D}}_{pl}(\omega; \mathbf{r}_0, \mathbf{r}_0) \cdot \mathbf{n}] \quad (1)$$

is the ET rate from QE to plasmon. Part of transferred energy is radiated away by the plasmonic antenna at rate that is determined by plasmon's radiation efficiency while the rest is dissipated in the metal. These processes are included in the plasmon Green function, which, for  $\omega$  close to plasmon frequency  $\omega_{pl}$ , has the form [37, 39]

$$\bar{\mathbf{D}}_{pl}(\omega; \mathbf{r}, \mathbf{r}') = \frac{\omega_{pl}}{4U_{pl}} \frac{\mathbf{E}(\mathbf{r}) \mathbf{E}(\mathbf{r}')}{\omega_{pl} - \omega - i\gamma_{pl}/2}, \quad (2)$$

where  $U_{pl}$  is the plasmon mode energy [57],

$$U_{pl} = \frac{1}{16\pi} \int dV \frac{\partial [\omega_{pl} \varepsilon'(\omega_{pl}, \mathbf{r})]}{\partial \omega_{pl}} \mathbf{E}^2(\mathbf{r}) \quad (3)$$

and  $\gamma_{pl} = W_{pl}/U_{pl}$  is the plasmon decay rate. Here,  $W_{pl} = W_{pl}^{nr} + W_{pl}^r$  is the power dissipated by plasmon due to nonradiative ( $W_{pl}^{nr}$ ) and radiative ( $W_{pl}^r$ ) losses. The Ohmic contribution to  $W_{pl}$  has the form [57]  $W_{pl}^{nr} = (\omega_{pl}/8\pi) \int dV \varepsilon''(\omega_{pl}, \mathbf{r}) \mathbf{E}^2(\mathbf{r})$ , where integration is, in fact, restricted to metallic regions with complex dielectric function  $\varepsilon(\omega) = \varepsilon'(\omega) + i\varepsilon''(\omega)$ . Since integration in  $U_{pl}$  is also restricted to such regions, the standard form for plasmon's nonradiative decay rate  $\gamma_{pl}^{nr} = W_{pl}^{nr}/U_{pl} = 2\varepsilon''(\omega_{pl})/[\partial \varepsilon'(\omega_{pl})/\partial \omega_{pl}]$  is recovered. At the same time, for system size smaller than radiation wavelength, the power *radiated* by plasmon is similar to that of localized dipole,  $W_{pl}^r = (\omega_{pl}^4/3c^3) \mathcal{P}^2$ , where  $\mathcal{P} = \int dV \mathbf{E}(\mathbf{r}) \chi(\omega_{pl}, \mathbf{r})$  is plasmon's dipole moment and  $\chi(\omega_{pl}, \mathbf{r}) = [\varepsilon'(\omega_{pl}, \mathbf{r}) - 1]/4\pi$  is plasmonic system susceptibility [37]. Accordingly, the plasmon radiative decay rate  $\gamma_{pl}^r = W_{pl}^r/U_{pl}$  determines the radiation efficiency of single-mode plasmonic antenna:  $\eta = \gamma_{pl}^r/(\gamma_{pl}^{nr} + \gamma_{pl}^r)$ .

The QE-plasmon ET rate is obtained by substituting

the plasmon Green function (2) into Eq. (1),

$$\gamma_{et}^c(\omega) = \frac{\mu^2 Q}{\hbar U_{pl}} \frac{[\mathbf{n} \cdot \mathbf{E}(\mathbf{r}_0)]^2}{1 + 4Q^2(\omega/\omega_{pl} - 1)^2}, \quad (4)$$

where  $Q = \omega_{pl}/\gamma_{pl}$  is the plasmon quality factor. The maximal enhancement of QE's decay rate at resonance  $\omega = \omega_{pl}$  is usually described as  $\gamma(\omega_{pl}) = \gamma_0^r(1+F)$ , where  $F$  is the Purcell factor. Introducing the plasmon mode volume at point  $\mathbf{r}$  projected along  $\mathbf{n}$  as [37]

$$\frac{1}{\mathcal{V}_n(\mathbf{r})} = \frac{2 [\mathbf{n} \cdot \mathbf{E}(\mathbf{r})]^2}{\int dV \mathbf{E}^2 \partial(\omega_{pl} \varepsilon')/\partial \omega_{pl}}, \quad (5)$$

the Purcell factor for plasmonic resonators takes the form

$$F = \frac{6\pi Q}{k^3 \mathcal{V}_n} = \frac{12\pi Q [\mathbf{n} \cdot \mathbf{E}(\mathbf{r}_0)]^2}{k^3 \int dV \mathbf{E}^2 \partial(\omega_{pl} \varepsilon')/\partial \omega_{pl}}, \quad (6)$$

where we denoted  $\varepsilon \equiv \varepsilon(\omega_{pl}, \mathbf{r})$  in the integrand. The enhancement factor for radiated power spectrum is  $M(\omega) = [\gamma_{et}(\omega)/\gamma_0^r]\eta$ , with maximal enhancement  $M(\omega_{pl}) = F\eta$ .

Let us now turn to light emission from *ensemble* of  $N$  excited QEs located at positions  $\mathbf{r}_i$  near plasmonic nanostructure. We assume incoherent excitation, i.e., QEs' dipole moments have the form  $\mathbf{p}_i = \mu \mathbf{n}_i e^{i\phi_i}$ , where  $\mathbf{n}_i$  are QEs' dipole orientations, assumed to be random, and  $\phi_i$  are random phases reflecting that QEs' initial states are uncorrelated. Each excited QE now couples to the *common* electric field as  $\mathbf{p}_i^* \cdot \mathbf{E}(\mathbf{r}_i)$ , where the field

$$\mathbf{E}(\mathbf{r}) = \sum_j \bar{\mathbf{D}}(\omega; \mathbf{r}, \mathbf{r}_j) \cdot \mathbf{p}_j, \quad (7)$$

is generated by *all* QEs, implying that the system eigenstates are determined by the Green function matrix between QEs' positions [43]:  $D_{ij} = \hbar^{-1} \mathbf{p}_i^* \cdot \bar{\mathbf{D}}(\omega; \mathbf{r}_i, \mathbf{r}_j) \cdot \mathbf{p}_j$ .

Following near-field decomposition of the dyadic Green function  $\bar{\mathbf{D}}$ , the coupling matrix  $\hat{D}$  can be split into free-space and plasmon parts,  $D_{ij} = D_{ij}^0 + D_{ij}^{pl}$ , where the plasmon coupling  $D_{ij}^{pl}$  describes plasmon-assisted correlations between QEs and, for QE frequencies close to  $\omega_{pl}$ , dominates over the free-space coupling  $D_{ij}^0$ . The latter accounts for direct (mostly dipole-dipole) interactions between QEs and can be neglected for now (we will discuss it later). With help of the plasmon Green function (2), the plasmon coupling matrix takes the form

$$D_{ij}^{pl}(\omega) = \frac{\omega_{pl}}{4\hbar U_{pl}} \frac{\mathbf{p}_i^* \cdot \mathbf{E}(\mathbf{r}_i) \mathbf{p}_j \cdot \mathbf{E}(\mathbf{r}_j)}{\omega_{pl} - \omega - i\gamma_{pl}/2}, \quad (8)$$

where diagonal elements  $D_{ii} = \delta\omega^i + i\gamma_{et}^i/2$  include frequency shifts  $\delta\omega^i$  and QE-plasmon ET rates  $\gamma_{et}^i$  for individual QEs [see Eq. (4)]. The eigenstates of matrix (8) describe collective states formed due to the plasmonic correlations between QEs, while the complex eigenvalues  $\lambda$  describe these states' frequency shifts and decay rates.

It is easy to see that the collective state represented by the vector  $\psi_c = \{\mathbf{p}_1^* \cdot \mathbf{E}_m(\mathbf{r}_1), \dots, \mathbf{p}_N^* \cdot \mathbf{E}_m(\mathbf{r}_N)\}$  is the

eigenstate of coupling matrix (8) that *saturates* ET from QEs to plasmon. Indeed, the corresponding eigenvalue has the form  $\delta\omega^c + i\gamma_{et}^c/2$ , where

$$\gamma_{et}^c = \sum_i \gamma_{et}^{(i)}, \quad \delta\omega^c = \sum_i \delta\omega^{(i)}, \quad (9)$$

are, respectively, the collective state's decay rate and frequency shift. The rest of eigenstates are uncoupled from the plasmon but, in principle, can radiate on their own.

Thus, we have established that, due to plasmonic correlations, a collective state of  $N$  excited QEs transfers its energy *cooperatively* at rate that equals the sum of individual QE-plasmon ET rates. Using Eq. (4) for individual rates, the CET rate takes the form

$$\gamma_{et}^c(\omega) = \frac{\mu^2 Q}{\hbar U_{pl}} \sum_i \frac{[\mathbf{n}_i \cdot \mathbf{E}(\mathbf{r}_i)]^2}{1 + 4Q^2(\omega/\omega_{pl} - 1)^2}. \quad (10)$$

Normalizing the CET rate at resonance  $\gamma_{et}^c(\omega_{pl})$  by  $\gamma_0^r$ , we obtain cooperative Purcell factor

$$F_c = \sum_i \frac{6\pi Q}{k^3 \mathcal{V}_n^{(i)}} = \sum_i \frac{12\pi Q_m |\mathbf{n}_i \cdot \mathbf{E}_m(\mathbf{r}_i)|^2}{k^3 \int dV |\mathbf{E}_m|^2 \partial(\omega_m \varepsilon')/\partial\omega_m} \quad (11)$$

as the sum of Purcell factors (6) for individual QEs.

Let us turn to power spectrum radiated by  $N$  excited QEs via CET to plasmonic antenna. The full radiated power  $W_r$  is obtained by integrating Poynting's vector  $\mathbf{S} = (c/8\pi)|\mathbf{E}(\mathbf{r})|^2$  over remote surface enclosing the system, where  $\mathbf{E}(\mathbf{r})$  is the far field generated by QEs. To extract the far field contribution from Eq. (7), we use the Dyson equation for Green function,  $\bar{\mathbf{D}} = \bar{\mathbf{D}}_0 + \bar{\mathbf{D}}_0 \cdot \chi \bar{\mathbf{D}}$ . Near the resonance, by replacing  $\bar{\mathbf{D}}$  with the plasmon Green function (2), we obtain after some algebra

$$W_r = \frac{\omega^4}{3c^3} \left| \sum_i \left[ \mathbf{p}_i + \frac{\omega_{pl}}{4U_{pl}} \frac{\mathbf{P}[\mathbf{E}(\mathbf{r}_i) \cdot \mathbf{p}_i]}{\omega_{pl} - \omega - i\gamma_{pl}/2} \right] \right|^2, \quad (12)$$

where the second term describes contribution of the antenna with dipole moment  $\mathbf{P}$ . After averaging out over random phases in  $\mathbf{p}_i = \mu \mathbf{n}_i e^{i\phi_i}$  and neglecting nonresonant direct QE emission (first term), we obtain radiated power spectrum mediated by CET to plasmonic antenna

$$W_r^c = \frac{\mu^2 \omega^4}{3c^3} \frac{\gamma_{pl}^r \gamma_{et}^c(\omega)}{\gamma_{pl} \gamma_0^r}, \quad (13)$$

where CET rate  $\gamma_{et}^c(\omega)$  is given by Eq. (10). Finally, the cooperative enhancement factor for radiated power spectrum is obtained by normalizing  $W_r^c$  with individual QE's radiated power  $W_r^0 = \mu^2 \omega^4 / 3c^3$  [56],

$$M_c(\omega) = \frac{W_r^c}{W_r^0} = \frac{F_c \eta}{1 + 4Q^2(\omega/\omega_{pl} - 1)^2}. \quad (14)$$

At resonance, the enhancement factor is  $M_c(\omega_{pl}) = F_c \eta$ .

*Discussion.*—A distinct feature of CET-based cooperative emission is its robust power spectrum that retains

plasmon resonance lineshape with overall amplitude scaling with the cooperative decay rate. This spectral stability contrasts common cooperative mechanisms, e.g., Dicke superradiance, where decay rate change directly affects the emission linewidth [43–47]. Furthermore, CET to plasmonic antenna is largely insensitive to QE frequency variations due to, e.g., direct dipole-dipole interactions, as long as they fit within broad plasmon resonance band, in contrast to, e.g., superradiance, where even weak disorder leads to drastic changes in the emission spectra [52, 53]. Also note that for large number of QEs, quenching effects that hinder single-QE emission near the metal surface are largely suppressed [59, 60].

We stress that CET-based cooperative emission is *weak* coupling effect that does not require plasmon reabsorption, unlike strong coupling regime characterized by coherent QE-plasmon energy exchange [14–20]. Excited QEs that are coupled to a *single* plasmon mode undergo CET if their *emission* spectrum overlaps with plasmon absorption band. If QE's absorption band is well above its emission peak, the energy transferred to plasmonic antenna is radiated away at rate that scales with the number of *excited* QEs involved in CET, which can be varied in wide range with excitation power.

Let us analyze CET scenarios for common QEs distributions near plasmonic structure. If QEs are placed in a *plasmonic cavity*, e.g., within dielectric core surrounded by metallic shell, the plasmon field is nearly uniform in the QE region, and so the mode volume  $\mathcal{V}_n^{(i)}$  in Eq. (16), which characterizes plasmon field localization at  $\mathbf{r}_i$ , is constant on average. In this case, the cooperative Purcell factor is simply  $F_c = NF$ , i.e., the ensemble spontaneous decay rate scales *linearly* with the excited QE number.

In another setup, QEs are placed *outside* the metal structure, e.g., within dielectric shell around metal core (see Fig. 1). In this case, plasmon fields decrease rapidly away from the metal surface. We assume uniform QE distribution, with random dipole orientations, in a region of volume  $V_0$  and dielectric constant  $\varepsilon_d$ . Introducing the average mode volume in the QE region as [61]

$$\frac{1}{V_0} = \frac{1}{V_0} \frac{2 \int dV_0 \mathbf{E}^2}{\int dV \mathbf{E}^2 \partial(\omega_{pl} \varepsilon')/\partial\omega_{pl}}, \quad (15)$$

the cooperative Purcell factor takes the form

$$F_c = \frac{2\pi N Q}{k^3 V_0} = \frac{4\pi n}{k^3} \frac{Q \int dV_0 \mathbf{E}^2}{\int dV \mathbf{E}^2 \partial(\omega_{pl} \varepsilon')/\partial\omega_{pl}}, \quad (16)$$

where  $n = N/V_0$  is QE concentration, and the extra factor  $1/3$ , compared to individual Purcell factor (6), comes from orientational averaging. Note that CET-based cooperativity is characterized by parameter  $N/V_0$ , i.e., QEs' number within average mode volume, rather than by common superradiance parameter  $N/V_0$  [42, 43].

Since remote QEs couple weakly to the plasmon, a sufficiently large QE region *saturates* the mode volume, i.e., no significant field spillover takes place beyond this region. In this case, the integrated field intensity  $\int dV_0 \mathbf{E}^2$

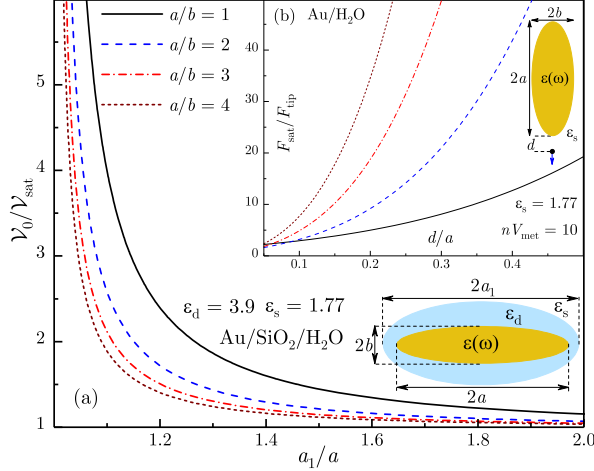


FIG. 2. (a) Average mode volume in units of saturated one is plotted vs. QE region size. (b) Cooperative enhancement vs. local field enhancement for QE at distance  $d$  from metal tip.

is independent of  $V_0$  and so the saturated mode volume  $\mathcal{V}_{\text{sat}}$  scales with  $V_0$ . Using the Gauss law and omitting the remote QEs' contribution [58], we obtain universal *field-independent* saturated plasmon mode volume,

$$\frac{\mathcal{V}_{\text{sat}}}{V_0} = \frac{\epsilon_d \omega_{pl}}{2|\epsilon'(\omega_{pl})|} \frac{\partial \epsilon'(\omega_{pl})}{\partial \omega_{pl}}, \quad (17)$$

which depends on system geometry only via plasmon frequency  $\omega_{pl}$  in the metal dielectric function. Finally, for saturated case, the cooperative Purcell factor (16) is

$$F_{\text{sat}} = \frac{2\pi NQ}{k^3 \mathcal{V}_{\text{sat}}} = \frac{4\pi nQ}{k^3 \epsilon_d} \frac{|\epsilon'(\omega_{pl})|}{\omega_{pl} \partial \epsilon'(\omega_{pl}) / \partial \omega_{pl}}. \quad (18)$$

Remarkably, cooperative Purcell factor for QE distribution saturating the plasmon mode volume is determined *solely* by experimentally measured system parameters.

As an example, we consider Au nanorods in water coated by QE-doped  $\text{SiO}_2$  shell modeled by two confocal prolate spheroids [see schematics in Fig. 2(a)]. The inner and outer surfaces correspond to semi-major axes  $a$  and  $a_1$ , respectively, and QE concentration  $n = N/V_0$  is constant within the shell volume  $V_0$  [58]. With extending QE region, i.e., increasing  $a_1/a$ , the average mode volume for longitudinal plasmon rapidly saturates, i.e.,  $\mathcal{V}_0/\mathcal{V}_{\text{sat}} \approx 1$  for relatively thin shells [see Fig. 2(a)].

In Fig. 2(b) we compare cooperative Purcell factor (18) to Purcell factor  $F_{\text{tip}}$  of a single QE placed near Au nanorod tip, where local fields are strongest [see schematics Fig. 2(b)]. Since plasmon mode volume near the tip scales with the metal volume  $V_{\text{met}}$  [37], the ratio  $F_{\text{sat}}/F_{\text{tip}}$  scales with  $nV_{\text{met}}$ , but is very sensitive to QE's distance  $d$  to the tip [58]. For relatively low value  $nV_{\text{met}} = 10$ , i.e., number of QEs that would fit within metal volume at given QE concentration  $n$  in the shell, the cooperative enhancement of decay rate far exceeds the local field enhancement. Note that for  $d < 1$  nm, the local fields are damped by nonlocal effects [40, 41].

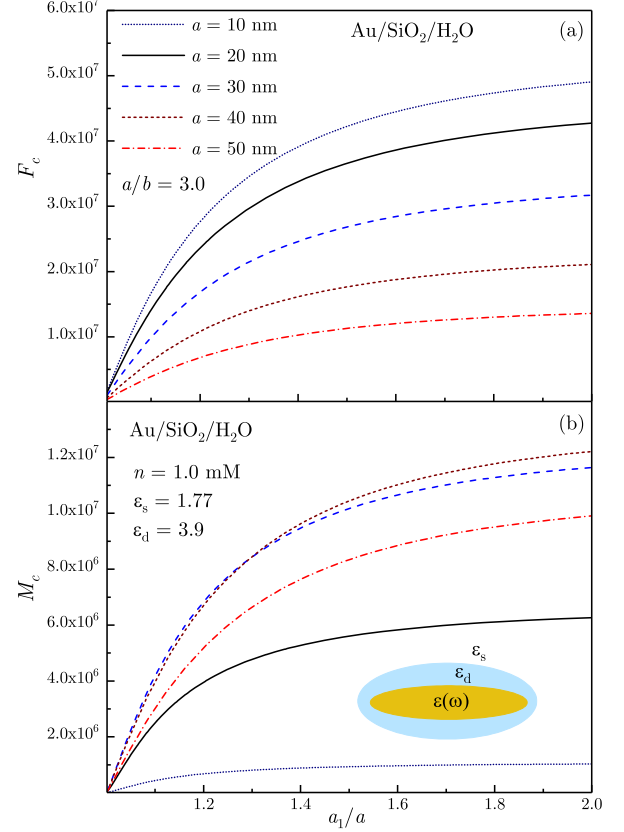


FIG. 3. Cooperative Purcell factor (a) and power spectrum enhancement factor (b) are plotted vs. QE region size with increasing nanorod length at fixed core aspect ratio  $a/b = 3.0$ .

In Fig. 3, we plot cooperative Purcell factor  $F_c$  and power spectrum enhancement factor  $M_c = F_c \eta$  vs. QE region size, with increasing nanorod length at fixed aspect ratio  $a/b = 3.0$ , and for QE concentration  $n = 1.0 \text{ mM}$ . Although the plasmon mode volume is nearly saturated at  $a_1/a = 2.0$  [see Fig. 2(a)], the curves still show weak size dependence due to plasmon frequency change with shell thickness. The evolution of  $F_c$  and  $M_c$  with nanorod length is defined by interplay between plasmon quality factor  $Q$  and radiation efficiency  $\eta$ , which change in opposite ways with increasing  $\gamma_{pl}^r$ . In fact, the smallest nanorod ( $a = 10$  nm) has the largest Purcell factor  $F_c \propto Q$  [see Fig. 3(a)] but, at the same time, the smallest enhancement factor  $M_c \propto Q\eta$ , while the largest  $M_c$  are those of medium-sized rods [see Fig. 3(b)]. Note that the optimal radiation efficiency for maximal power spectrum enhancement is  $\eta = 1/2$ .

In summary, we described new mechanism for cooperative emission of light by an ensemble of excited QEs mediated by cooperative energy transfer to the plasmonic antenna. The cooperative emission rate scales with the number of excited QEs and, for large ensembles saturating the plasmon mode volume, has universal form independent of local field distribution in the system.

This work was supported in part by NSF grants No. DMR-1610427 and No. HRD-1547754.

---

[1] S. A. Maier, *Plasmonics: Fundamentals and Applications*, (Springer, New York, 2007).

[2] M. Moskovits, Rev. Mod. Phys. **57** 783 (1985) .

[3] S. A. Maier and H. A. Atwater, J. Appl. Phys. **98**, 011101 (2005).

[4] E. Ozbay, Science **311**, 189 (2006).

[5] M. I. Stockman, in *Plasmonics: Theory and Applications*, edited by T. V. Shahbazyan and M. I. Stockman (Springer, New York, 2013).

[6] E. C. Le Ru and P. G. Etchegoin, *Principles of Surface-Enhanced Raman Spectroscopy* (Elsevier, 2009).

[7] P. Anger, P. Bharadwaj, and L. Novotny, Phys. Rev. Lett. **96**, 113002 (2006).

[8] S. Kühn, U. Hakanson, L. Rogobete, and V. Sandoghdar, Phys. Rev. Lett. **97**, 017402 (2006).

[9] F. Tam, G. P. Goodrich, B. R. Johnson, and N. J. Halas, Nano Lett. **7**, 496 (2007).

[10] J. R. Lakowicz, J. Kusba, Y. Shen, J. Malicka, S. DAuria, Z. Gryczynski, I. Gryczynski, J. Fluoresc. **13**, 69 (2003).

[11] P. Andrew and W. L. Barnes, Science **306**, 1002 (2004).

[12] F. Reil, U. Hohenester, J. R. Krenn, and A. Leitner, Nano Lett. **8**, 4128 (2008).

[13] C. Blum, N. Zijlstra, A. Lagendijk, M. Wubs, A. P. Mosk, V. Subramaniam, W. L. Vos, Phys. Rev. Lett. **109**, 203601 (2012).

[14] J. Bellessa, C. Bonnand, J. C. Plenet, and J. Mugnier, Phys. Rev. Lett. **93**, 036404 (2004).

[15] Y. Sugawara, T. A. Kelf, J. J. Baumberg, M. E. Abdelsalam, and P. N. Bartlett, Phys. Rev. Lett. **97**, 266808 (2006).

[16] N. T. Fofang, T.-H. Park, O. Neumann, N. A. Mirin, P. Nordlander, and N. J. Halas, Nano Lett. **8**, 3481 (2008).

[17] D. E. Gomez, K. C. Vernon, P. Mulvaney, and T. J. Davis, Nano Lett. **10**, 274 (2010).

[18] A. Salomon, R. J. Gordon, Y. Prior, T. Seideman, and M. Sukharev, Phys. Rev. Lett. **109**, 073002 (2012).

[19] S. Aberra Guebrou, C. Symonds, E. Homeyer, J. C. Plenet, Y. N. Gartstein, V. M. Agranovich, and J. Bellessa, Phys. Rev. Lett. **108**, 066401 (2012).

[20] T. Antosiewicz, S. P. Apell, and T. Shegai, ACS Photonics, **1**, 454 (2014).

[21] D. J. Bergman and M. I. Stockman, Phys. Rev. Lett., **90**, 027402, (2003).

[22] M. I. Stockman, Nature Photon. **2**, 327, (2008).

[23] M. A. Noginov, G. Zhu, A. M. Belgrave, R. Bakker, V. M. Shalaev, E. E. Narimanov, S. Stout, E. Herz, T. Suteewong and U. Wiesner, Nature, **460**, 1110, (2009).

[24] M. Pelton, Nat. Photon. **9**, 427 (2015).

[25] G. M. Akselrod, C. Argyropoulos, T. B. Hoang, C. Ciraci, C. Fang, J. Huang, D. R. Smith, and M. H. Mikkelsen, Nat. Photon. **8**, 835 (2014).

[26] M. S. Eggleston, K. Messer, L. Zhan, E. Yablonovitch, M. C. Wu, Proc. Nat. Acad. Sci., **112**, 1704 (2015).

[27] F. D. Angelis, M. Malerba, M. Patrini, E. Miele, G. Das, A. Toma, R. P. Zaccaria, E. D. Fabrizio, Nano Lett. **13**, 3553 (2013).

[28] C.-Y. Jin, R. John, M. Y. Swinkels, T. B. Hoang, L. Midolo, P. J. van Veldhoven, A. Fiore, Nat. Nanotechnol. **9**, 886 (2014).

[29] M. Malerba, A. Alabastri, E. Miele, P. Zilio, M. Patrini, D. Bajoni, G. C. Messina, M. Dipalo, A. Toma, R. P. Zaccaria, F. D. Angelis, Sci. Rep. **5**, 16436 (2015).

[30] P. Guo, R. D. Schaller, J. B. Ketterson, and R. P. H. Chang, Nat. Photon. **10**, 267 (2016).

[31] R. Carminati, J. J. Greffet, C. Henkel, J. M. Vigoureux, Opt. Commun. **261** 368 (2006).

[32] C. Sauvan, J. P. Hugonin, I. S. Maksymov, and P. Lalanne, Phys. Rev. Lett. **110**, 237401 (2013).

[33] A. E. Krasnok, A. P. Slobozhanyuk, C. R. Simovski, S. A. Tretyakov, A. N. Poddubny, A. E. Miroshnichenko, Y. S. Kivshar, and P. A. Belov, Sci. Rep. **5**, 12956 (2015).

[34] F. Marquier, C. Sauvan, and J.-J. Greffet, ACS Phot. **4**, 20912101 (2017).

[35] A. F. Koenderink, ACS Phot. **4**, 710-722 (2017).

[36] P. Lalanne, W. Yan, K. Vynck, C. Sauvan, and J.P. Hugonin, Laser Photon. Rev. **12**, 1700113 (2018).

[37] T. V. Shahbazyan, arXiv:1805.09529.

[38] E. M. Purcell, Phys. Rev. **69** 681 (1946).

[39] T. V. Shahbazyan, Phys. Rev. Lett. **117**, 207401 (2016).

[40] C. Ciraci, R. T. Hill, J. J. Mock, Y. Urzumov, A. I. Fernndez-Domnguez, S. A. Maier, J. B. Pendry, A. Chilkoti, and D. R. Smith, Science **337**, 1072 (2012).

[41] N. A. Mortensen, S. Raza, M. Wubs, T. Søndergaard, and S. I. Bozhevolnyi, Nat. Commun. **5**, 3809 (2014).

[42] R. H. Dicke, Phys. Rev. **93**, 99 (1954).

[43] M. Gross and S. Haroche, Phys. Rep. **93**, 301 (1982).

[44] V. N. Pustovit, T. V. Shahbazyan, Phys. Rev. Lett. **102**, 077401 (2009).

[45] V. N. Pustovit, T. V. Shahbazyan, Phys. Rev. B **82**, 075429 (2010).

[46] D. Martin-Cano, L. Martin-Moreno, F. J. Garcia-Vidal, and E. Moreno, Nano Lett. **10**, 3129 (2010).

[47] J. J. Choquette, K.-P. Marzlin, and B. C. Sanders, Phys. Rev. A **82**, 023827 (2010).

[48] V. N. Pustovit, A. M. Urbas, T. V. Shahbazyan, Phys. Rev. B **88**, 245427 (2013).

[49] Y. Zhang and V. May, Phys. Rev. B **89**, 245441 (2014).

[50] N. J. Schilder, C. Sauvan, J.-P. Hugonin, S. Jennewein, Y. R. P. Sortais, A. Browaeys, and J.-J. Greffet, Phys. Rev. A **93**, 063835 (2016).

[51] P. Fauchè, S. G. Kosionis, and P. Lalanne, Phys. Rev. B **95**, 195418 (2017).

[52] R. Friedberg, S. R. Hartmann, and J. T. Manassah, Phys. Rep. C **7**, 101 (1973).

[53] T. V. Shahbazyan, M. E. Raikh, and Z. V. Vardeny, Phys. Rev. B **61**, 13266 (2000).

[54] L. N. Tripathi, M. Praveena, and J. K. Basu, Plasmonics, **8**, 657 (2013).

[55] M. V. Shestakov, E. Fron, L. F. Chibotaru, and V.V. Moshchalkov, J. Phys. Chem. C **119**, 20051 (2015).

[56] L. Novotny and B. Hecht, *Principles of Nano-Optics* (CUP, New York, 2012).

[57] L. D. Landau and E. M. Lifshitz, *Electrodynamics of Continuous Media* (Elsevier, Amsterdam, 2004).

[58] See Supplemental Material.

[59] A. Delga, J. Feist, J. Bravo-Abad, and F.J. Garcia-Vidal, Phys. Rev. Lett. **112**, 253601 (2014).

[60] L. S. Petrosyan and T. V. Shahbazyan, Phys. Rev. B **96**, 075423 (2017).

[61] T. V. Shahbazyan, ACS Photon. **4**, 1003 (2017).